Monthly Notices
of the
ROYAL ASTRONOMICAL SOCIETY

MNRAS **447,** 3526–3535 (2015) doi:10.1093/mnras/stu2726

The rich are different: evidence from the RAVE survey for stellar radial migration

G. Kordopatis,[1,2★] J. Binney,[3] G. Gilmore,[1] R. F. G. Wyse,[4] V. Belokurov,[1] P. J. McMillan,[3] P. Hatfield,[1,5] E. K. Grebel,[6] M. Steinmetz,[2] J. F. Navarro,[7†] G. Seabroke,[8] I. Minchev,[2] C. Chiappini,[2] O. Bienaymé,[9] J. Bland-Hawthorn,[10] K. C. Freeman,[11] B. K. Gibson,[12,13] A. Helmi,[14] U. Munari,[15] Q. Parker,[16,17,18] W. A. Reid,[16,17] A. Siebert,[8] A. Siviero[19] and T. Zwitter[20]

[1]*Institute of Astronomy, University of Cambridge, Madingley Road, Cambridge CB3 0HA, UK*
[2]*Leibniz-Institut für Astrophysik Potsdam (AIP), An der Sternwarte 16, D-14482 Potsdam, Germany*
[3]*Rudolf Peierls Centre for Theoretical Physics, Keble Road, Oxford OX1 3NP, UK*
[4]*Johns Hopkins University, Homewood Campus, 3400 N Charles Street, Baltimore MD 21218, USA*
[5]*Department of Physics, University of Oxford, Denys Wilkinson Building, Keble Road, Oxford OX1 3RH, UK*
[6]*Astronomisches Rechen-Institut, Zentrum für Astronomie der Universität Heidelberg, Mönchhofstr. 12–14, D-69120 Heidelberg, Germany*
[7]*Department of Physics and Astronomy, University of Victoria, Victoria BC V8P 5C2, Canada*
[8]*Mullard Space Science Laboratory, University College London, Holmbury St Mary, Dorking RH5 6NT, UK*
[9]*Observatoire astronomique de Strasbourg, Université de Strasbourg, CNRS, UMR 7550, 11 rue de l'Université, F-67000 Strasbourg, France*
[10]*Sydney Institute for Astronomy, School of Physics A28, University of Sydney, NSW 2611, Australia*
[11]*RSAA Australian National University, Mount Stromlo Observatory, Cotter Road, Weston Creek, Canberra, ACT 72611, Australia*
[12]*Institute for Computational Astrophysics, Department of Astronomy & Physics, Saint Mary's University, Halifax, NS BH3 3C3, Canada*
[13]*Jeremiah Horrocks Institute, University of Central Lancashire, Preston PR1 2HE, UK*
[14]*Kapteyn Astronomical Institute, University of Groningen, PO Box 800, NL-9700 AV Groningen, the Netherlands*
[15]*INAF Astronomical Observatory of Padova, I-36012 Asiago (VI), Italy*
[16]*Department of Physics and Astronomy, Macquarie University, Sydney, NSW 2109, Australia*
[17]*Research Centre in Astronomy, Astrophysics and Astrophotonics, Macquarie University, Sydney, NSW 2109, Australia*
[18]*Australian Astronomical Observatory, PO Box 915, North Ryde, NSW 1670, Australia*
[19]*Department of Physics and Astronomy, Padova University, Vicolo dell'Osservatorio 2, I-35122 Padova, Italy*
[20]*Faculty of Mathematics and Physics, University of Ljubljana, 1000 Ljubljana, Slovenia*

Accepted 2014 December 19. Received 2014 December 19; in original form 2014 September 29

ABSTRACT

Using the RAdial Velocity Experiment fourth data release (RAVE DR4), and a new metallicity calibration that will be also taken into account in the future RAVE DR5, we investigate the existence and the properties of supersolar metallicity stars ($[M/\mathrm{H}] \gtrsim +0.1$ dex) in the sample, and in particular in the solar neighbourhood. We find that RAVE is rich in supersolar metallicity stars, and that the local metallicity distribution function declines remarkably slowly up to +0.4 dex. Our results show that the kinematics and height distributions of the supersolar metallicity stars are identical to those of the $[M/\mathrm{H}] \lesssim 0$ thin-disc giants that we presume were locally manufactured. The eccentricities of the supersolar metallicity stars indicate that half of them are on a roughly circular orbit ($e \leq 0.15$), so under the assumption that the metallicity of the interstellar medium at a given radius never decreases with time, they must have increased their angular momenta by scattering at corotation resonances of spiral arms from regions far inside the solar annulus. The likelihood that a star will migrate radially does not seem to decrease significantly with increasing amplitude of vertical oscillations within range of oscillation amplitudes encountered in the disc.

Key words: Galaxy: abundances – Galaxy: disc – Galaxy: evolution – Galaxy: kinematics and dynamics – Galaxy: stellar content.

1 INTRODUCTION

The disc is our Galaxy's dominant visible component and contains most of the baryons that lie within a sphere of radius $r \sim 100$ kpc.

★E-mail: gkordo@ast.cam.ac.uk
†CIfAR Senior Fellow.

Hence, if we are to understand how our very typical Galaxy has arisen within the Λ cold dark matter paradigm (Springel, Frenk & White 2006), we need to know how the disc is structured, functions and was formed. Since the seminal works of Spitzer & Schwarzschild (1953), Pagel & Patchett (1975), Matteucci & Francois (1989) and others, the relevant framework has been recognized to be the accretion of cool gas on to a centrifugally supported disc within which stars form on nearly circular orbits. Dying stars enrich the star-forming gas with metals, and fluctuations in the Galaxy's gravitational field cause stars to migrate to less circular orbits that are more inclined to the Galactic plane (Binney 2013; Sellwood 2014, and references therein).

In a classic study, Eggen, Lynden-Bell & Sandage (1962) showed that the orbits of the stars and the chemical composition of their atmospheres suggest how one may reconstruct the history of the Milky Way. While the chemical composition of a star retains (to a good approximation) an imprint of the chemistry of the interstellar medium (ISM) at the time and place of its birth (e.g. Yoshii 1981; Freeman & Bland-Hawthorn 2002), its orbit depends both on the environment in which the star formed (within circularly orbiting gas or gas in free fall, or the gas disc of a satellite) and subsequent evolution of the orbit in response to fluctuations in the Galaxy's gravitational field (generated by molecular clouds, spiral structure, the bar, halo substructure, etc.). The correlations between chemistry and kinematics are therefore tracers of the coevolution of nucleosynthesis and dynamical evolution.

The component L_z of angular momentum about the Galaxy's approximate symmetry axis plays a crucial role, and with L_z we associate a guiding centre radius r_g by the equation $L_z = r_g v_c(r_g)$, where $v_c(r)$ is the speed of a circular orbit at r. A star with angular momentum L_z executes radial oscillations around r_g. Changes in L_z are therefore associated with changes in r_g and one speaks of 'radial migration' when L_z changes.

Measurements of the abundances and metallicities[1] of young O and B stars, and nebular abundances, reveal the chemistry of the current ISM, whereas measurements of lower mass FGK stars, reveal the chemistry of the ISM billions of years in the past. The available data are consistent with the conjecture that within a given Galactocentric annulus; the ISM is chemically homogeneous. In particular, the ISM is very homogeneous within several hundred parsecs of the Sun (Cartledge et al. 2006). So if we could establish the ISM's radial metallicity profile $[M/\mathrm{H}]_\tau(R)$ for each time τ in the past, we could infer the birth radius of a star of age τ from its measured value of $[M/\mathrm{H}]$ (see Boeche et al. 2013b; Gazzano et al. 2013; Hayden et al. 2014, and references therein for radial metallicity gradients of FGK stars).

Stars in the solar neighbourhood with metallicities above solar ($[M/\mathrm{H}] > 0$) are especially powerful probes of the evolution of the Milky Way's disc. They can form only after several previous generations of stars have enriched their local ISM (e.g. Pagel 1997; Matteucci 2003). This can either take several billion years in regions where the star formation rate is low and approximately constant with time (OB stars in the Milky Way disc near the Sun only reach, on average, $[M/\mathrm{H}] = 0$; Nieva & Przybilla 2012), or occur rapidly in dense environments, such as the Galactic bulge, where we find stars with $[M/\mathrm{H}] > 0$ that are several billion years old (e.g. Whitford & Rich 1983; Hill et al. 2011).

[1] We denote the overall metallicity of a star, $[M/\mathrm{H}]$, the ratio of the abundance of any element to its abundance in the Sun. It is defined as $[M/\mathrm{H}] = \log(M/\mathrm{H})_\star - \log(M/\mathrm{H})_\odot$.

Given the homogeneity of the ISM, stars with $[M/\mathrm{H}] \gtrsim 0.15$ dex (noted super metal-rich stars, SMR stars, hereafter) must have formed inside the Sun's Galactocentric distance R_0, and we see them here either because they have significantly increased their Galactocentric angular momenta, and thus their guiding-centre radii (Grenon 1989, 1999; Chiappini 2009), or because they have moved to significantly eccentric orbits or on account of a combination of both these processes.

Sellwood & Binney (2002) showed that the dominant effect of transient spiral structure is to cause stars that are in corotation resonance (CR) with the spiral to exchange angular momentum without changing the eccentricity of their orbits. They dubbed this process 'churning'. Lynden-Bell & Kalnajs (1972) had already shown that stars that are in a Lindblad resonance exchange angular momentum with the spiral in such a way that on average they move to more eccentric orbits: at inner Lindblad resonance (ILR) stars typically surrender angular momentum to the spiral, while at outer Lindblad resonance (OLR) they gain angular momentum from the spiral. Since stars scattered at ILR lose angular momentum, and the great majority of disc stars were born inside R_0 (which is of order 3 of the disc's exponential scalelengths), SMR stars on highly eccentric orbits are likely to have been scattered at OLR and thus have increased both their angular momenta and eccentricity.

Hence, a star that has markedly increased its angular momentum without moving to a highly eccentric orbit must have been scattered at CR by the churning process. The azimuthal velocities of these stars will not lag the circular velocity by much. On the other hand, stars that reach the Sun on eccentric orbits from guiding centres that are significantly smaller than R_0 will lag the local circular speed significantly. Hence by measuring the random velocities and the azimuthal speeds of stars, we should be able to determine the relative importance of scattering at CR and at OLR.

The observational evidence for radial migration is still relatively scanty. In nearby disc galaxies, Yoachim, Roškar & Debattista (2012) and Radburn-Smith et al. (2012) measured for a subsample of their targets a change of the age of the dominant population at the location of the break in the disc surface brightness, in agreement with the theoretical work of Roškar et al. (2008) on broken exponential profile in galaxies experiencing radial migration. As far as the Milky Way is concerned, Sellwood & Binney (2002) and Haywood (2008) argued that the large scatter in the age–metallicity relation near the Sun (e.g. Edvardsson et al. 1993; Bergemann et al. 2014) is evidence of radial migration, whereas Lee et al. (2011), using *SEGUE* data (*Sloan Extension for Galactic Understanding and Exploration*; Yanny et al. 2009), invoked radial migration to explain why the metallicity of thin disc stars (for the range $-0.5 \lesssim [\mathrm{Fe/H}] \lesssim +0.2$ dex) is uncorrelated with their orbital eccentricity. Finally, using RAdial Velocity Experiment data (RAVE data; Steinmetz et al. 2006), Minchev et al. (2014b) found a decline of the velocity dispersion of the α-enhanced low-metallicity disc stars, and suggested that the stars responsible for this decline are migrators from the inner disc.

The actual efficiency of radial migration, i.e. the maximum distance from which a star can reach the solar neighbourhood, has never been observationally constrained. Indeed, this is a challenging task, since distinguishing radially migrated stars from ones of the same metallicity that were born locally requires either accurate ages (for example, SMR stars having migrated from the bulge region should be on average older than locally born stars at the same metallicity) or knowing how the metallicity gradient of the ISM has evolved. In this paper, however, we aim to obtain a first

estimate of the radial migration efficiency by investigating the shape of the metallicity distribution function (MDF) of the metal-rich tail of the solar-neighbourhood stars, in combination with a study of stellar orbits. For this purpose, we use the kinematically unbiased spectroscopic catalogue of RAVE (Steinmetz et al. 2006), for which the latest data release (DR4; Kordopatis et al. 2013a) has published the atmospheric parameters, metallicities and distances of approximately 400 000 relatively bright FGK stars ($9 < I < 12$ mag).

Section 2 describes the data set used, in particular the new calibration of the metal-rich end, as well as the way the distances, velocities and orbits of the stars have been computed. Section 3 characterizes the significance of the SMR stars that we identify in RAVE, and shows that the normal disc giants is likely to have amongst them stars born in regions where the Galactic bulge now dominates. Finally, Section 4 concludes.

2 DESCRIPTION OF THE DATA AND THE NEW METALLICITY CALIBRATION RELATION

2.1 A new metallicity calibration for the metal-rich stars

One of the major improvements of RAVE DR4 (Kordopatis et al. 2013a), compared to the previous data releases (Zwitter et al. 2008; Siebert et al. 2011), is its more thorough metallicity calibration, based on the RAVE observations of cluster stars and the availability of high-resolution spectra of already observed RAVE targets. Although the calibration has had several successes (e.g. Kordopatis et al. 2013b; Binney et al. 2014; Conrad et al. 2014; Kordopatis 2014; Minchev et al. 2014b), it suffered from a lack of calibration targets at the high-metallicity end. High-metallicity stars are not α-rich, so at the high-metallicity end the [M/H] and [Fe/H] distributions should approximately coincide. In Fig. 1, the black histogram shows the DR4 [M/H] distribution while the green histogram shows the [Fe/H] distribution from the RAVE chemical pipeline (Boeche et al. 2013a). Contrary to expectation, the [M/H] distribution falls far below the [Fe/H] distribution at the high-metallicity end.

In the light of this discrepancy, the RAVE DR4 metallicity calibration has been revised at the metal-rich end, using spectra of Gaia Benchmark stars (Jofré et al. 2014) processed through the RAVE pipeline, as well as a comparison of the pipeline's results for an additional 150 metal-rich stars that had parameters derived from very high resolution spectra using the High Accuracy Radial velocity Planet Searcher spectrograph (HARPS; Adibekyan et al. 2013) and the Fiber-fed Extended Range Optical Spectrograph (FEROS; Worley et al. 2012). Details of the updated calibration will be given in the RAVE-DR5 paper (in preparation). In summary, the calibration procedure is the same as in DR4, i.e. fitting the difference between the metallicities derived from the pipeline and literature metallicities of all available calibrators to a second-order polynomial in $\log g$ and [M/H]. The resulting calibration relation is almost unchanged for all of the stars with $[M/\mathrm{H}] \lesssim 0$ (less than $\sim$0.05 dex difference), and provides a more symmetric shape of the MDF at $[M/\mathrm{H}] > 0$ the red histogram of Fig. 1 shows the new distribution.

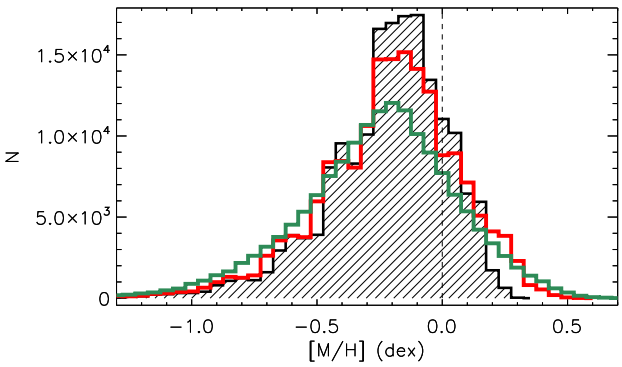

Figure 1. Metallicity distributions of the selected RAVE quality subsample. The x-axis shows the DR4 metallicities (black histogram), the DR5 metallicities (red histogram) or the iron abundance ([Fe/H], green histogram) coming from the DR4 chemical pipeline. The y-axis shows the number of RAVE stars, N, in each bin. [A colour version of this figure is available in the online version.]

2.2 Distances, positions, orbits and quality subsample

After modifying the metallicities of the stars, one should redetermine the distances to these stars since the DR4 distances (Binney et al. 2014) used the DR4 metallicities. However, by re-running the distance pipeline it has been found that increasing the metallicities of all supersolar metallicity stars by up to +0.15 dex typically adds $\sim$0.05 to the derived distance moduli (see Fig. 2). This represents about a 2 per cent increase in distance, which is negligible compared to our uncertainties, estimated to be $\sim$15 per cent. Hence, here we use the published DR4 distances.

We adopted the solar motion with respect to the local standard of rest (LSR) of Schönrich, Binney & Dehnen (2010), namely $U_0 = 11.1$, $V_0 = 12.24$ and $W_0 = 7.25\,\mathrm{km\,s^{-1}}$, and assumed that the Sun is located at $(R_0, Z_0) = (8, 0)$ kpc and that the LSR is on a circular orbit with circular speed $V_c = 220\,\mathrm{km\,s^{-1}}$. Then from the DR4 data we computed the Galactocentric positions and velocities of the stars, in the same way as in Kordopatis et al. (2013b).

We used the model Galaxy of Dehnen & Binney (1998), where the Galactic gravitational potential is built with three superposed double-exponential discs (thin disc, thick disc and gas layer) and two spheroids (bulge and dark halo). More specifically, the density of each disc is given by

$$\rho(R,z) = \frac{\Sigma_0}{2z_\mathrm{d}} \exp\left[-\left(\frac{R_\mathrm{h}}{R} + \frac{R}{R_\mathrm{d}} + \frac{|z|}{z_\mathrm{d}}\right)\right], \quad (1)$$

where R and z are the coordinates in a Galactocentric cylindrical coordinate system, R_d and z_d are, respectively, the scalelength and

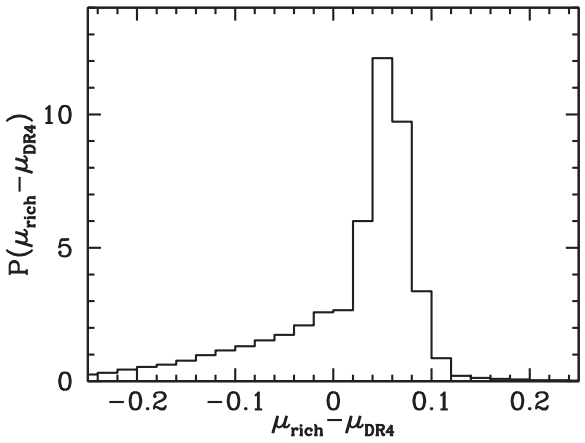

Figure 2. Probability density $(1/\mu)$ of the change in the distance modulus of the metal-rich stars when their DR4 metallicity is increased by 0.15 dex, which is the maximum effect that DR5 metallicity calibration has on DR4 metallicities. The mean effect is an increase of 0.05 in the distance modulus, which translates into an increase of about 2 per cent in the derived line-of-sight distances.

Table 1. Parameters for the adopted mass model of the Milky Way.

Disc	Thick	Thin	Gas
Σ_0 ($M_\odot$ kpc^{-2})	7.30×10^7	1.11×10^9	1.14×10^8
R_d(kpc)	2.4	2.4	4.8
z_d(kpc)	1.0	0.36	0.04
R_h(kpc)	0	0	4
Spheroid	Dark halo	Bulge	
ρ_0 ($M_\odot$ kpc^{-3})	1.26×10^9	7.56×10^8	
q	0.8	0.6	
γ	−2	1.8	
β	2.21	1.8	
r_0(kpc)	1.09	1	
r_{cut}(kpc)	1000	1.9	

scaleheight, Σ_0 is the disc's central surface density and where a non-zero value of R_h generates a central depression in the disc. The density of the spheroids is given by

$$\rho(R,z) = \frac{\rho_0}{m^\gamma (a+m)^{\beta-\gamma}} \exp[-(mr_0/r_{cut})^2], \quad (2)$$

where β and γ control the outer and inner density slopes, r_0 and r_{cut} are the scale and cut-off radii, ρ_0 sets the scale density and m, defined as

$$m(R,z) \equiv \sqrt{(R/r_0)^2 + (z/qr_0)^2}, \quad (3)$$

includes the axial ratio q of the isodensity surfaces. Table 1 presents the values that are adopted in this work for each disc and spheroid. In the fixed potential of this model, we used the 'Stäckel Fudge' of Binney (2012) to determine the smallest r_p and largest r_a radii at which the orbit defined by its given initial condition cuts the Galactic plane, and then computed the orbit's mean radius $\overline{r} \equiv (r_p + r_a)/2$ and the orbital eccentricity $e \equiv (r_a - r_p)/(r_a + r_p)$.

The sample analysed here is selected to have reliable stellar parameters (and therefore distances, velocities and orbits) following the recommendations of Kordopatis et al. (2013a). It contains only stars that have effective temperature T_{eff} >4000 K, surface gravity $\log g > 0.5$ dex, errors in line-of-sight velocity $eV_\parallel < 10\,\mathrm{km s^{-1}}$, spectral morphological flags set to '*n*' (normal stars) and for which the stellar parameter pipeline had converged.[2] In addition, we selected, for higher accuracy, only stellar parameters obtained from spectra with a signal-to-noise ratio (S/N) higher than 20.

3 CHARACTERIZATION OF THE METAL-RICH POPULATION

3.1 Identification of the strength of the signal

Fig. 1 shows the distributions of the DR4 metallicity (black points) and iron (green points) abundances for the selected quality sample; the red points show the distribution obtained with the new calibration (DR5). One can see the effect of the new DR5 calibration for the supersolar metallicity stars: they are now in better agreement with [Fe/H] in the shape of the tail of the distribution. In particular, one can notice that the selected RAVE quality subsample has more than 4×10^4 stars with $[M/H] > 0$. A visual inspection of the fit of the synthetic templates to the observed spectra confirmed that the results were in good agreement with the data (Fig. 3), and that

[2] Given the S/N threshold applied, algo_conv = 0 was required, indicating that the pipeline should converge without getting outside the synthetic spectra grid boundaries (see also Kordopatis et al. 2011).

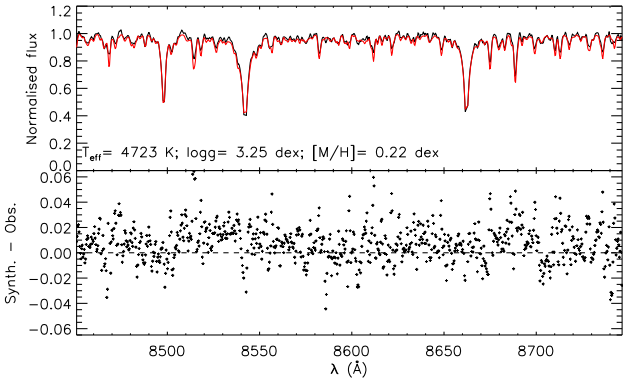

Figure 3. Top: observed (in black) and synthetic (in red) spectra of a RAVE super metal-rich star. Bottom: residuals between the observations and the synthetic spectrum. [A colour version of this figure is available in the online version.]

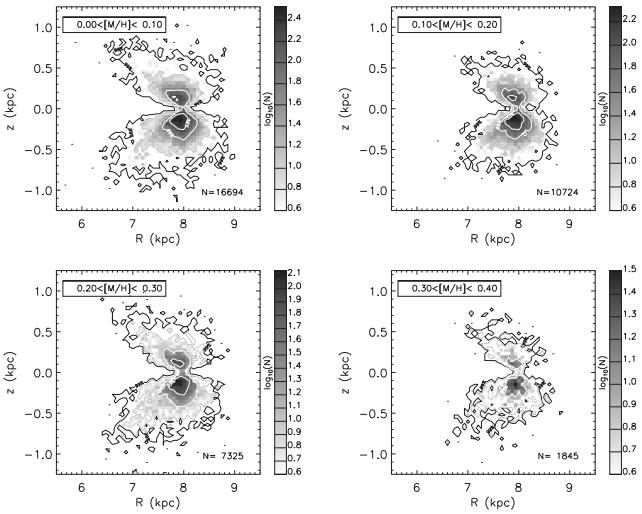

Figure 4. Positions of the metal-rich stars (in bins of 0.1 dex) in the (R, z) plane. The grey-scale is the logarithmic number of the targets. Most of targets are confined within 0.5 kpc of the Galactic plane, with however a non-negligible number reaching distances up to 1 kpc.

within the errors we could trust the derived parameters (see Kordopatis et al. 2013a, for a discussion on the internal errors of the method). These targets, all of which have $\log g \geq 2$ dex, are located relatively close to the Sun ($R = 8 \pm 1.5$ kpc, Fig. 4), and are mainly located near the Galactic plane, with nevertheless, some stars seen up to 1 kpc.

Fig. 5 shows that the MDF has roughly the same shape in the inner ($R < 8$ kpc) and outer ($R > 8$ kpc) Galaxy, although the inner Galaxy is marginally more metal-rich. However, we now ask to what extent the number of stars measured to be metal rich is boosted by stars scattered by observational error from the subsolar peak of the metallicity distribution ($[M/H] \sim -0.15$ dex, see Fig. 1). Suppose the uncertainty of the subsolar metallicity stars follows a Gaussian distribution, of standard deviation 0.1 dex, as suggested in tables 1 and 2 of Kordopatis et al. (2013a). Then the red dotted Gaussian of Fig. 5 indicates that only a small fraction of the stars with measured $[M/H] > 0.2$ dex would be generated by accidental scattering of subsolar stars. Indeed, the number of stars seen at $[M/H] > 0.05$ dex cannot be explained by accidental scattering even when the errors are overestimated by 50 per cent by setting $\sigma = 0.15$ dex (red solid Gaussian in Fig. 5).

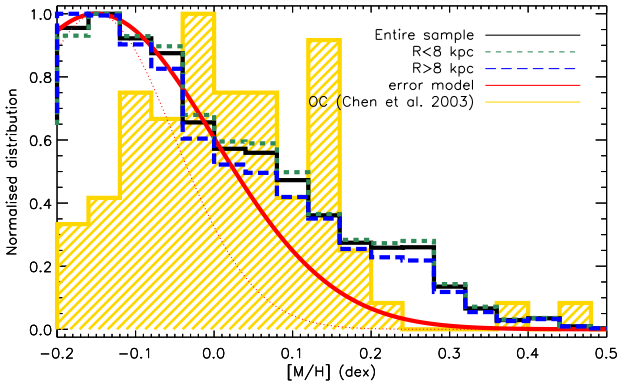

Figure 5. Normalized MDF of the metal-rich stars for the entire quality sample (black), the inner Galaxy one (green) and outer Galaxy one (blue). The MDF of 82 open clusters (out of 118 published by Chen et al. 2003), in the distance range $7.5 < R < 10$ kpc, is also illustrated in yellow. Finally, the red Gaussians have standard deviations of 0.1 (dashed line) and 0.15 dex (solid line) and represent the published and an overestimated internal error of the DR4 metallicity determination, respectively. [A colour version of this figure is available in the online version.]

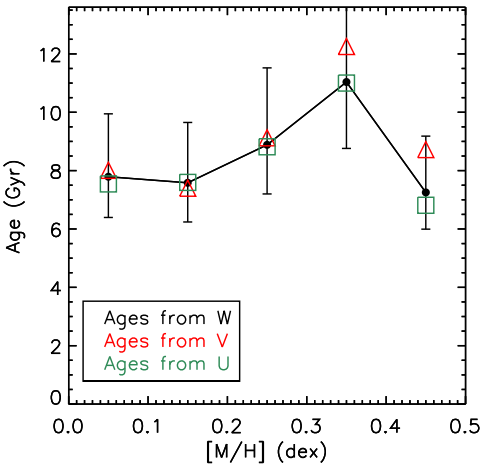

Figure 6. Age estimation of the metal-rich stars using the age–velocity dispersion relations for the U, V, W heliocentric velocity components. All age estimators are consistent with these being old stars. [A colour version of this figure is available in the online version.]

To further assess the plausibility of metal-rich stars really existing, in Fig. 5 we compare our $[M/H]$ distribution with the [Fe/H] distribution of the 82 open clusters published in Chen, Hou & Wang (2003) that have Galactocentric radii in the range probed by RAVE ($7.5 < R < 10$ kpc, yellow histogram). The metallicity distribution of the clusters is narrower than that of the stars, having its principal peak at $[M/H] \simeq 0$ rather than $[M/H] \simeq -0.17$ dex, and, with the exception of two outliers, falling to zero at $[M/H] = 0.2$ dex. The paucity of clusters with $[M/H] < 0$ is a natural consequence of the monotonic increase with time in the ISM's metallicity and the youth of clusters – the clusters are in the majority younger than 1.5 Gyr (Chen et al. 2003) whereas the RAVE metal-rich stars should be a few billion years old given the typical age (∼5 Gyr) of solar-metallicity field stars. The presence of old field stars more metal-rich than any but the two outlying clusters would be hard to explain in the absence of radial migration because the cluster distribution implies that even now, and more so in the past, in the probed radial range the gas is too metal-poor to form these stars.

We obtained a *rough* estimation of the age of the RAVE stars by applying, for different metallicity bins, the age–velocity dispersion relation defined for the heliocentric U, V, W velocities as

$$\sigma = a \times \mathrm{age}^k, \tag{4}$$

where σ is the velocity dispersion (σ_U, σ_V or σ_W), a is the local normalization factor, set in order to be equal to the velocity dispersion of 1-Gyr-old stars, and k is power-law exponent defining the age–velocity dispersion law. By adopting the values $(a_U, a_V, a_W) = (27, 18, 10)$ kms^{-1} (Robin et al. 2003) and $(k_U, k_V, k_W) = (0.31, 0.34, 0.47 \pm 0.05)$ (Nordström et al. 2004), we confirm the previous statement that the metal-rich stars in our sample are on average old (see Fig. 6), with approximate ages $\sim 8 \pm 2$ Gyr. We note that the age uncertainties are expected to be larger, as they depend on the values adopted for the parameters a and k in equation (4) (see table 8 of Sharma et al. 2014, for a review of the possible values of k). Our argument is simply that if the stars under study were young, their velocity dispersions would be significantly smaller than they actually are.

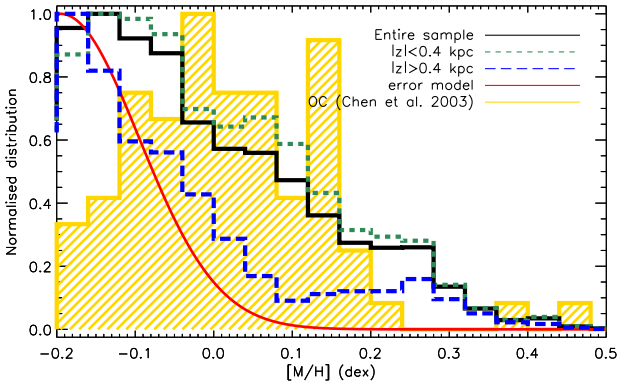

Figure 7. Same as Fig. 5, but for a separation as a function of the distance from the Galactic plane. The error model is a Gaussian of $\sigma = 0.1$ dex, centred at the peak of the blue histogram, at $[M/H] = -0.2$ dex. [A colour version of this figure is available in the online version.]

3.2 Identification of the radially migrated stars

As division of the sample by Galactocentric radius did not reveal any significant difference in the shape of the MDFs, in Fig. 7 we split our sample into closer and farther than 0.4 kpc from the plane[3] (note that given the RAVE footprint on the sky, stars far from the plane are preferentially located towards the inner Galaxy, see Fig. 4 and Kordopatis et al. 2013a).

The metallicity distributions of Fig. 7 indicate that an uncertainty of 0.15 dex in metallicity, as assumed above, is indeed an overestimation of the internal errors, since the high-altitude sample (blue broken curve) shows a narrower distribution in $[M/H]$. As discussed in the previous section, an uncertainty of 0.05–0.1 dex is more realistic.

Whereas the metallicity distribution of stars near the plane (green histogram) falls smoothly from a peak at $[M/H] \sim -0.125$ dex to near zero at $[M/H] \sim 0.5$ dex, that of stars farther than 0.4 kpc from the plane (blue histogram) falls smoothly from a peak at

[3] Other threshold values have been tested, up to 0.8 kpc in order to have enough stars in each subsample, without changing our conclusions.

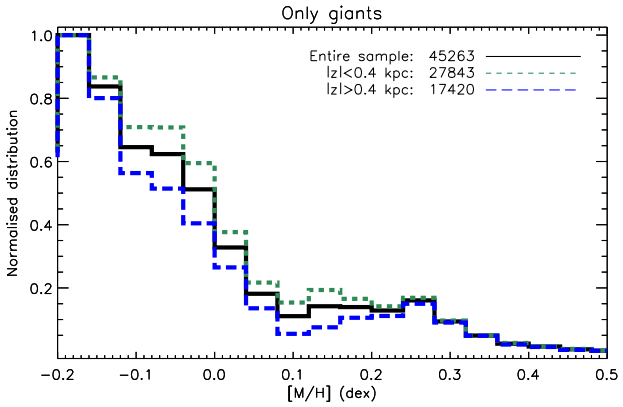

Figure 8. Same as Fig. 7, but only for stars with $\log g < 3.5$ dex. For $[M/\mathrm{H}] > 0.1$ dex, the metallicity distribution is flat for both the subsamples: that close to the plane and that far from it. [A colour version of this figure is available in the online version.]

$[M/\mathrm{H}] \sim -0.175$ dex to a local minimum at $[M/\mathrm{H}] \sim 0.1$ dex and then flattens to a very extensive tail. The tail rises to a peak around $[M/\mathrm{H}] = 0.275$ dex and then gradually fades. From $[M/\mathrm{H}] = 0.15$ dex the tail comprises the SMR stars.

In Fig. 8 the histograms show the metallicity distributions of just the giants ($\log g < 3.5$ dex): the green histogram is for those that lie closer than 0.4 kpc to the plane, the blue histogram for those further than 0.4 kpc from the plane and the black histogram is for the joint sample. The blue histogram differs little from that shown in Fig. 7 because all the contributing stars are quite distant and are unlikely to make the magnitude cut if they are not giants. But the sample of stars that are close to the plane is substantially modified by restricting the sample to giants, and we see that the metallicity distribution of the giants is essentially the same near and far from the plane. That is, in Fig. 7 the difference between the blue and black histograms is attributable by the contribution of the dwarfs. Many of the dwarfs are younger than the giants,[4] so they tend to be more metal-rich. Fig. 8 reveals that the metallicity distribution of the in-plane giants has a long tail to match that of the giants that are further away. Of course this is physically essential because most of the giants that are currently near the plane will in ∼50 Myr be far from it, and vice versa.

The key finding is that the (near-plane) dwarfs do not contribute significantly above 0.25 dex even though they are typically younger. If these SMR stars formed near us, we would expect them to have formed recently and include RAVE dwarfs. This is clearly not the case, at least for $[M/\mathrm{H}] \gtrsim 0.25$ dex.

The natural explanation of the tail is that it is made up of stars that have migrated to us from smaller radii, where high metallicities were achieved very early on (e.g. fig. 3 of Minchev, Chiappini & Martig 2013). The distance that the stars on the metal-rich end of the tail need to have travelled to match the observations, depends on the rate at which the disc enriched its metallicity at each radius over time (see for example Wyse & Silk 1989; Chiappini, Matteucci & Gratton 1997). The likelihood of an individual star reaching the solar neighbourhood decreases with distance to travel. However, the exponential rise inwards in the number of stars available to make the journey will to an extent compensate for the decreasing probability of coming far, with the result that the number in the tail decreases remarkably slowly with increasing $[M/\mathrm{H}]$. Future work will include developing such a model and investigating its plausibility in the light of the results of this study.

[4] Only a few young giants are expected to be present in our selection, due to their relatively short lifetime in that evolutionary phase.

3.3 Orbits of metal-rich stars

We now examine the orbits of the metal-rich stars. Fig. 9 and Table 2 illustrate and quantify the shape of the eccentricity distribution of the stars for three different distance ranges from the Galactic Centre and for different metallicity bins, starting from $[M/\mathrm{H}] \geq -0.2$ dex. Fig. 10 shows the mean orbital radii for the same stars. From these two figures, one can see that

(i) most of the stars have eccentricities below $e \approx 0.3$, with a peak at around $e \sim 0.15$ indicating, as expected for thin disc targets, that the stars are on nearly circular orbits.

(ii) No systematic variation is evident of the eccentricity distribution with metallicity. In particular, SMR stars are not more likely that low-metallicity stars to be on eccentric orbits.

(iii) There is a slight tendency for stars to be observed nearer apocentre than pericentre ($R > \bar{r}$). This bias towards apocentre may increase slightly with metallicity, but the effect is at best weak. Given that the density of stars decreases exponentially with guiding-centre radius, it is inevitable that when we focus on nearby stars with large eccentricities, stars with small guiding centres outnumber stars with large guiding centres, so the majority of stars with high eccentricities will be seen nearer apocentre than pericentre. Indeed most of the solar-neighbourhood stars with $e \geq 0.3$ prove to have mean orbital radii $\bar{r} \lesssim 6$ kpc. Thus, 'blurring' by eccentric orbits that have been populated by scattering at Lindblad resonances plays a significant role in bringing these stars to us. We will see, however, that the mean radii of these stars are too large to be their birth radii: even these stars have increased their angular momenta since birth.

Based on the values presented in Table 2 and illustrated in Fig. 9, the central row of Table 3 gives for different metallicity bins the proportion of giant stars of a given metallicity in the solar neighbourhood that are on nearly circular orbits ($e \lesssim 0.15$). This ratio proves to be roughly constant, of the order of 0.51. This is in agreement with Lee et al. (2011), who found that the thin disc stars have eccentricities that are independent of metallicity. In particular, we find that supersolar metallicity stars are not distributed differently in either eccentricity and or mean orbital radius from the stars of lower metallicity.

Taking into account (i) that supersolar metallicity stars are more metal-rich than the local ISM, (ii) that they are not a young population and (iii) that they are on nearly circular orbits, we can infer that these stars have increased their angular momenta through resonant scattering at CR. A quantitative theoretical estimate of the probable birth radii of solar vicinity stars with $[M/\mathrm{H}] > 0.2$ dex is given by Minchev et al. (2013) and Minchev, Chiappini & Martig (2014a). According to their simulations, these SMR stars would originate from the 3–5 kpc galactocentric region and would be at most 6 Gyr old. From the observational point of view, we can say that the present abundance gradient in the ISM, according to the most precise estimates based on Cepheids (e.g. Genovali et al. 2014), is around -0.06 dex kpc^{-1}. Although it is very unlikely that the gradient remained constant in the last 6–8 Gyr, this would imply that $[M/\mathrm{H}] = +0.4$ could be reached already at 2 kpc from the Galactic Centre under the assumption of a linear gradient.

Fig. 11 represents an illustration of the possible birth radii of any metallicity star, for two local metallicity gradients in the ISM,

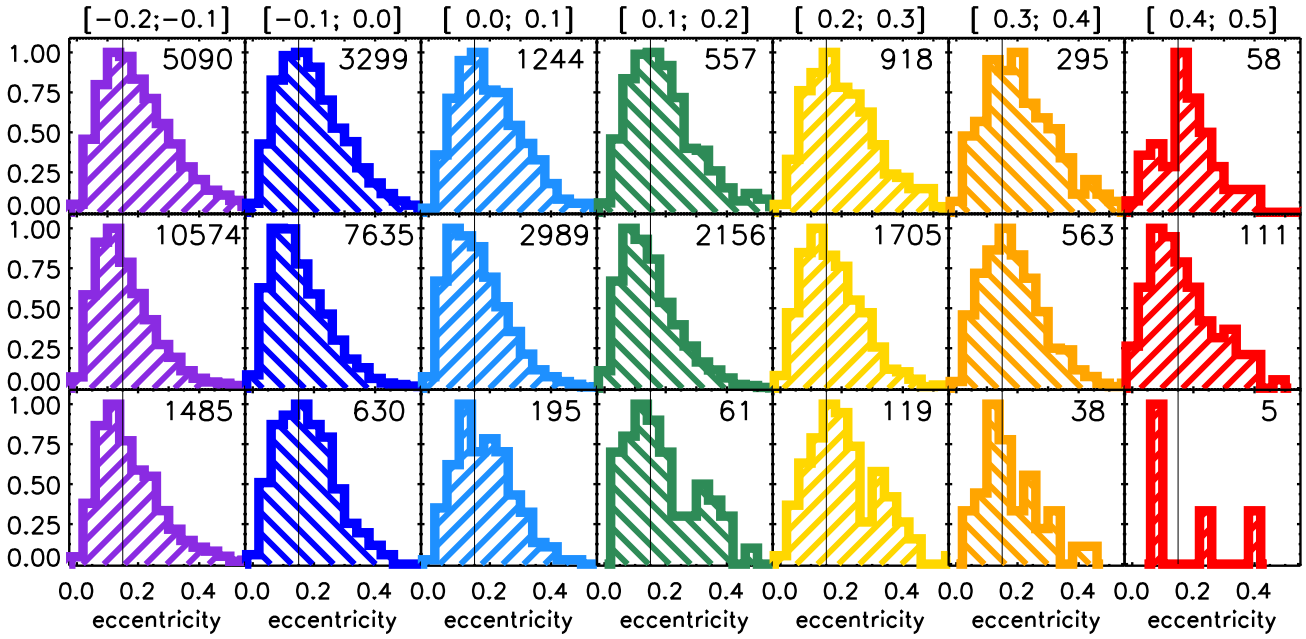

Figure 9. Eccentricity distribution (normalized to 1) of the RAVE giants quality subsample in the inner Galaxy ($6.5<R<7.5$ kpc, top), in the solar neighbourhood ($7.5<R<8.5$ kpc, middle) and in the outer Galaxy ($8.5<R<9.5$ kpc, bottom). The histograms are obtained for stars of increasing metallicity, in 0.1 dex wide bins, starting from −0.2 dex. For each histogram, the total number of stars considered is noted in the upper-right corner (the histograms have been truncated to $e = 0.55$). The plain vertical line in each panel is at $e = 0.15$, below which a star is considered having a circular orbit. The median and interquartile values of the distributions are reported in Table 2. [A colour version of this figure is available in the online version.]

Table 2. Median and interquartile values of the eccentricity distribution of the selected RAVE giants quality sample at three Galactocentric regions.

Metallicity range (dex)	[−0.2, −0.1]	[−0.1, 0.0]	[0.0, 0.1]	[0.1, 0.2]	[0.2, 0.3]	[0.3, 0.4]	[0.4, 0.5]
$6.5 < R < 7.5$	$0.18^{+0.28}_{-0.12}$	$0.18^{+0.26}_{-0.11}$	$0.19^{+0.28}_{-0.12}$	$0.18^{+0.26}_{-0.11}$	$0.19^{+0.28}_{-0.12}$	$0.20^{+0.29}_{-0.12}$	$0.18^{+0.24}_{-0.13}$
$7.5 < R < 8.5$	$0.14^{+0.21}_{-0.09}$	$0.14^{+0.21}_{-0.09}$	$0.14^{+0.22}_{-0.09}$	$0.13^{+0.20}_{-0.08}$	$0.16^{+0.23}_{-0.10}$	$0.18^{+0.25}_{-0.12}$	$0.14^{+0.23}_{-0.09}$
$8.5 < R < 9.5$	$0.16^{+0.24}_{-0.10}$	$0.17^{+0.24}_{-0.11}$	$0.18^{+0.25}_{-0.11}$	$0.16^{+0.27}_{-0.10}$	$0.19^{+0.29}_{-0.13}$	$0.16^{+0.25}_{-0.12}$	$0.10^{+0.25}_{-0.07}$

considering the extreme case in which $[M/\mathrm{H}]$ increases exponentially inwards with a scalelength R_M:

$$[M/\mathrm{H}](R) = A\left(1 - \mathrm{e}^{-(R-R_0)/R_\mathrm{M}}\right). \quad (5)$$

The constant A in this formula is the value to which $[M/\mathrm{H}]$ tends at large radii, and together with the value of local metallicity gas gradient, sets the value of R_M. Regardless of the adopted value of A, the shallowness of the local metallicity gradient in the ISM always implies $R < 3.5$ kpc for stars as metal rich as $[M/\mathrm{H}] = 0.4$

The first and third rows of Table 3 give $N_\mathrm{circ}/N_\mathrm{total}$ for the cylindrical shell inside and outside the solar cylinder, respectively. In these shells RAVE does not see stars that lie close to the plane (Fig. 4), so only warmer populations are sampled. Hence, it is no surprise that in these shells we find smaller values of $N_\mathrm{circ}/N_\mathrm{total}$ than in the solar cylinder: in the inner shell we have $N_\mathrm{circ}/N_\mathrm{total} \approx 0.36$ while in the outer shell we have $N_\mathrm{circ}/N_\mathrm{total} \approx 0.44$. However, the measured ratios still show no statistically significant variation over the entire investigated metallicity range (see Figs 9 and 10). Below we discuss how the lack of dependence of $N_\mathrm{circ}/N_\mathrm{total}$ on [Fe/H], even well off the plane can put constraints in the Galaxy's spiral history.

The gravitational field of a spiral structure that has radial wavenumber k varies with z as $\exp(-k|z|)$ (e.g. Binney & Tremaine 2008, section 6.1.5), so the capacity of a wave to force stars does not extend further than $1/k$ from the plane. Among the recent literature, disc simulations of spirals with different radial wavenumbers resulted to different observational predictions on radial migration. For example, the disc simulations of Solway, Sellwood & Schönrich (2012) were seeded with spiral arms through the groove mechanism of Sellwood & Kahn (1991) and in these simulations the extent of radial migration decreased only slowly with the amplitude of vertical excursions, and was 'almost as large for thick-disc stars as for those in the thin disc'. On the other hand, in the simulations of Vera-Ciro et al. (2014) the spirals were seeded by point masses in the disc intended to represent giant molecular clouds, and it was found, by contrast, that migrated stars were 'a heavily biased subset of stars with preferentially low vertical velocity dispersions'. This finding reflects the short wavelength, filamentary nature of the spiral structure in the discs of Vera-Ciro et al. (2014, see their fig. 2), which strongly confines the gravitational field to the equatorial plane.

The lack of dependence of $N_\mathrm{circ}/N_\mathrm{total}$ that we measure in our Galaxy implies that the responsible spiral structure has longer radial scales than that discussed by Vera-Ciro et al. (2014). This is consistent with K-band photometry of nearby face-on spiral galaxies that shows that the mass-bearing populations of these galaxies are organized into loosely wound spirals (Rix & Zaritsky 1995, Plate 1). A spiral structure, possibly groove driven like our results

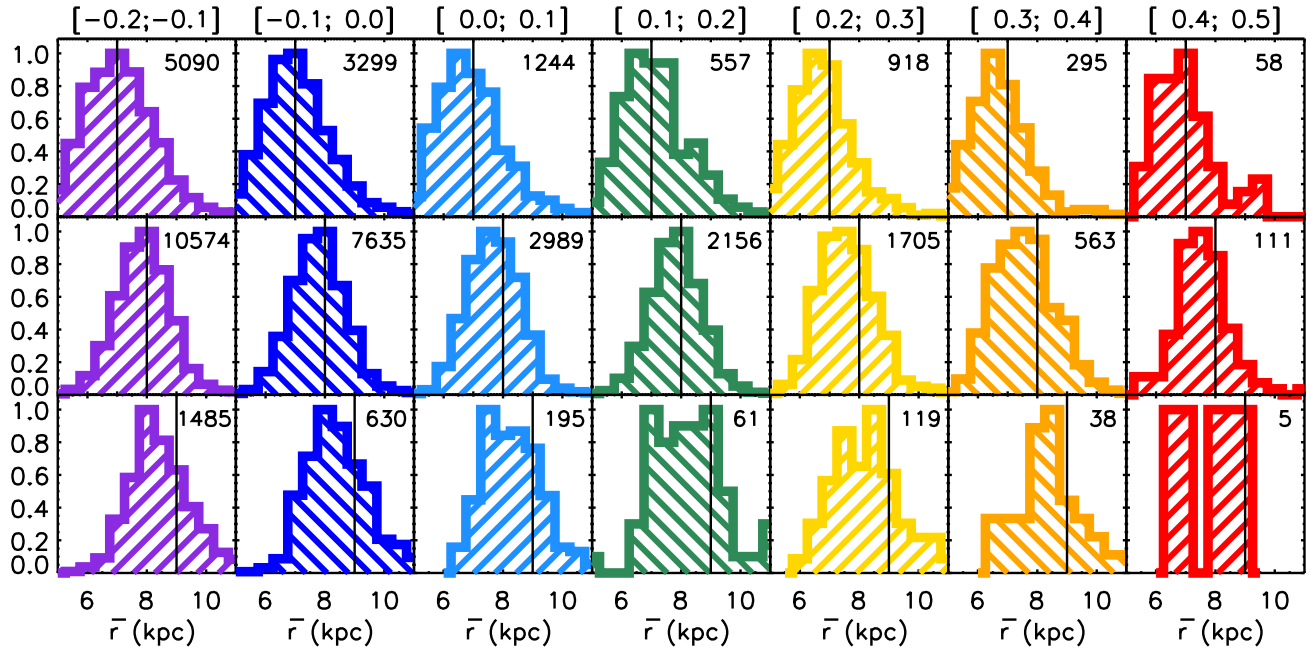

Figure 10. Same as for Fig. 9, but for the distribution of the mean orbital radius ($\bar{r}$) of the stars. In each panel, the plain vertical line is at the mean observed radius. Histograms have been truncated at [5, 11] kpc. [A colour version of this figure is available in the online version.]

Table 3. Ratio of circular orbit giant stars in the selected RAVE quality sample at three Galactocentric regions.

Metallicity range (dex)		[−0.2, −0.1]	[−0.1, 0.0]	[0.0, 0.1]	[0.1, 0.2]	[0.2, 0.3]	[0.3, 0.4]	[0.4, 0.5]
$N_{\rm circ}/N_{\rm total}$	$6.5 < R < 7.5$	0.38	0.39	0.36	0.39	0.35	0.35	0.31
	$7.5 < R < 8.5$	0.54	0.55	0.53	0.57	0.46	0.40	0.52
	$8.5 < R < 9.5$	0.47	0.42	0.41	0.41	0.33	0.47	0.60

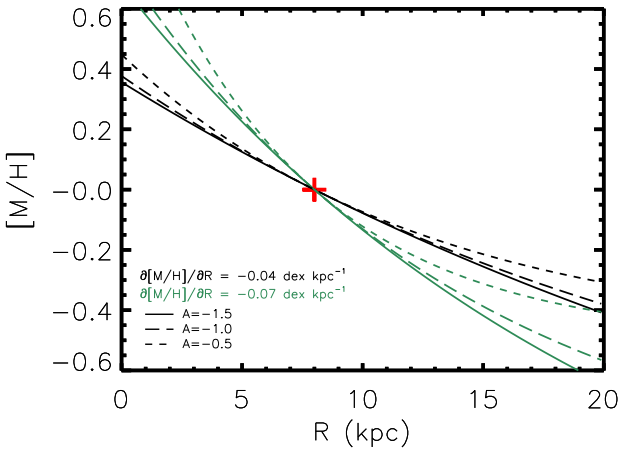

Figure 11. Example of an extreme steepening of the metallicity gradient of the ISM, following an exponential form (see equation 5). Different metallicity values at high radii (factor A) and locally measured ISM metallicity gradients are adopted to illustrate possible ranges of birth locations of the stars. The red '+' sign is at (R_0, [M/H]) = (8 kpc, 0). [A colour version of this figure is available in the online version.]

suggest, is also in agreement with Sellwood & Carlberg (2014) that have argued that the groove mechanism is fundamental to the development of large-amplitude spiral structure in discs that contain only stars and are stable at the level of linear perturbation theory.

4 DISCUSSION AND CONCLUSIONS

A recalibration of the metallicities of stars in the RAVE survey leads to a significant increase in the number of stars with [M/H] > 0.2 dex and brings the metallicity distribution of the entire RAVE sample into closer agreement with that of the DR4 chemical pipeline. In fact the two distributions are now in good agreement for [M/H] > 0.1 dex.

Currently the ISM has metallicity [M/H] < 0 near the Sun, and its metallicity increases towards the Galactic Centre, the local gas gradient being of the order of d[M/H]/d$R \simeq -0.06$ dex kpc^{-1} (e.g. Smartt & Rolleston 1997; Balser et al. 2011; Genovali et al. 2014). In the absence of large amounts of metal-poor gas being accreted, the natural expectation for gas metallicity at a given radius is to be a monotonic increasing function of time, so current metallicities give upper limits on metallicities at all previous times (e.g. Chiappini 2009). If these propositions are accepted and one grants that the metallicity of a star reflects the metallicity of the ISM at the time and place of its formation, it follows that SMR stars with [M/H] ∼ 0.4 dex must have formed far inside R_0, probably in the region now occupied by the bar/bulge.

Indeed, the alternative scenario of these stars forming *in situ* nearer the Sun, from a turbulent ISM that has reached [M/H] ∼ 0.4 dex at early times seems unlikely, because turbulence extensive enough to mix gas from the inner galaxy to $R = 6$ kpc (where the stellar metallicity gradient measured for example by the APOGEE survey becomes flatter) requires clouds to be on significantly non-circular orbits, and in such clouds few stars would

be born on to the near-circular orbits on which we observe many SMR stars. Moreover, realistic turbulent discs as seen in external galaxies at $z \sim 1$–2 (Epinat et al. 2012; Tacconi et al. 2013) are too short lived (e.g. Genzel et al. 2008; Bournaud, Elmegreen & Martig 2009) to allow enriched inner galactic ISM to reach outer galactic regions.

We have shown that SMR stars are not on particularly eccentric orbits. It follows that they have materially increased their angular momenta through resonant scattering by spiral arms (Sellwood & Binney 2002), and most no longer visit the region of their birth. Angular momentum can be increased at either CR or OLR, and the key distinction between these resonances is that at OLR eccentricity increases, while at CR it does not. Since the SMR stars have experienced large angular momentum increases without large increases in eccentricity, it follows that the dominant process bringing them to us is scattering at CR, i.e. churning.

We have shown that the vertical distribution of the higher metallicity stars is not unusual. In fact, as far as we can determine, the spatial distribution of these stars is independent of metallicity. The natural interpretation of this finding is that the probability for radial migration is insensitive to the extent of a star's excursions perpendicular to the plane. This interpretation is consistent with the dynamical study of Solway et al. (2012), who showed an example of a disc seeded with spiral structure through the groove mechanism of Sellwood & Kahn (1991) where migration probability is almost as large for thick-disc stars as for those in the thin disc. Our interpretation of the data implies that the radial wavelength of spiral structure is no smaller than the thick disc's scaleheight, which is not the case in the experiments of Vera-Ciro et al. (2014) who used a simulation with multi-armed recurrent spirals and showed that churning is far more efficient for stars with low vertical velocity dispersion.

Finally, we note that rather than radial migration, the SMR stars could be evidence of inhomogeneous chemical evolution within the Galactic disc on account of the Galactic fountain (e.g. Marasco, Marinacci & Fraternali 2013, and references therein) bringing metal-rich ejecta from an interior region of the disc to somewhere in the solar annulus and there giving rise to metal-rich star formation (Spitoni et al. 2009). However, this scenario seems implausible because (i) the ratio of stars on nearly circular and eccentric orbits is independent of metallicity, and (ii) high-velocity clouds, which may be associated with the Galactic fountain, have low metallicities (Wakker 2001). However, only a few hundred high-resolution spectra of SMR stars should be enough to identify their chemical abundance patterns and test this possibility. Large and high-resolution surveys such as *Gaia*-ESO (Gilmore et al. 2012) or APOGEE (Allende Prieto et al. 2008) could, perhaps, already provide some answers to the above questions.

ACKNOWLEDGEMENTS

The anonymous referee is greatly thanked for the useful comments and suggestions that helped improving the quality of this paper. Funding for RAVE has been provided by: the Australian Astronomical Observatory; the Leibniz-Institut für Astrophysik Potsdam (AIP); the Australian National University; the Australian Research Council; the French National Research Agency; the German Research Foundation (SPP 1177 and SFB 881); the European Research Council (ERC-StG 240271 Galactica); the Instituto Nazionale di Astrofisica at Padova; The Johns Hopkins University; the National Science Foundation of the USA (AST-0908326); the W. M. Keck foundation; the Macquarie University; the Netherlands Research School for Astronomy; the Natural Sciences and Engineering Research Council of Canada; the Slovenian Research Agency; the Swiss National Science Foundation; the Science & Technology Facilities Council of the UK; Opticon; Strasbourg Observatory and the Universities of Groningen, Heidelberg and Sydney. RFGW acknowledges support of NSF Grant OIA-1124403 and thanks the Aspen Center for Physics and NSF Grant no. 1066293 for hospitality during the writing of this paper. The research leading to these results has received funding from the European Research Council under the European Union's Seventh Framework Programme (FP7/2007-2013)/ERC grant agreement no. 321067. The RAVE website is at http://www.rave-survey.org.

REFERENCES

Adibekyan V. Z. et al., 2013, A&A, 554, A44
Allende Prieto C. et al., 2008, Astron. Nachr., 329, 1018
Balser D. S., Rood R. T., Bania T. M., Anderson L. D., 2011, ApJ, 738, 27
Bergemann M. et al., 2014, A&A, 565, A89
Binney J., 2012, MNRAS, 426, 1324
Binney J., 2013, New Astron. Rev., 57, 29
Binney J., Tremaine S., 2008, Galactic Dynamics, 2nd edn. Princeton Univ. Press, Princeton, NJ
Binney J. et al., 2014, MNRAS, 437, 351
Boeche C. et al., 2013a, A&A, 553, A19
Boeche C. et al., 2013b, A&A, 559, A59
Bournaud F., Elmegreen B. G., Martig M., 2009, ApJ, 707, L1
Cartledge S. I. B., Lauroesch J. T., Meyer D. M., Sofia U. J., 2006, ApJ, 641, 327
Chen L., Hou J. L., Wang J. J., 2003, AJ, 125, 1397
Chiappini C., 2009, in Andersen J., Nordström B., Bland-Hawthorn J., eds, Proc. IAU Symp. 254, The Galaxy Disk in Cosmological Context. Cambridge Univ. Press, Cambridge, p. 191
Chiappini C., Matteucci F., Gratton R., 1997, ApJ, 477, 765
Conrad C. et al., 2014, A&A, 562, A54
Dehnen W., Binney J., 1998, MNRAS, 294, 429
Edvardsson B., Andersen J., Gustafsson B., Lambert D. L., Nissen P. E., Tomkin J., 1993, A&A, 275, 101
Eggen O. J., Lynden-Bell D., Sandage A. R., 1962, ApJ, 136, 748
Epinat B. et al., 2012, A&A, 539, A92
Freeman K., Bland-Hawthorn J., 2002, ARA&A, 40, 487
Gazzano J.-C., Kordopatis G., Deleuil M., de Laverny P., Recio-Blanco A., Hill V., 2013, A&A, 550, A125
Genovali K. et al., 2014, A&A, 566, A37
Genzel R. et al., 2008, ApJ, 687, 59
Gilmore G. et al., 2012, The Messenger, 147, 25
Grenon M., 1989, Ap&SS, 156, 29
Grenon M., 1999, Ap&SS, 265, 331
Hayden M. R. et al., 2014, AJ, 147, 116
Haywood M., 2008, MNRAS, 388, 1175
Hill V. et al., 2011, A&A, 534, A80
Jofré P. et al., 2014, A&A, 564, A133
Kordopatis G., 2014, in Ballet J., Martins F., Bournaud F., Monier R., Reylé C., eds, SF2A-2014: Proc. Annual meeting of the French Society of Astronomy and Astrophysics. Société Francaise d'Astronomie et d'Astrophysique, Paris, p. 431
Kordopatis G., Recio-Blanco A., de Laverny P., Bijaoui A., Hill V., Gilmore G., Wyse R. F. G., Ordenovic C., 2011, A&A, 535, A106
Kordopatis G. et al., 2013a, AJ, 146, 134
Kordopatis G. et al., 2013b, MNRAS, 436, 3231
Lee Y. S. et al., 2011, ApJ, 738, 187
Lynden-Bell D., Kalnajs A. J., 1972, MNRAS, 157, 1
Marasco A., Marinacci F., Fraternali F., 2013, MNRAS, 433, 1634
Matteucci F., 2003, The Chemical Evolution of the Galaxy. Kluwer, Dordrecht
Matteucci F., Francois P., 1989, MNRAS, 239, 885

Minchev I., Chiappini C., Martig M., 2013, A&A, 558, A9
Minchev I., Chiappini C., Martig M., 2014a, A&A, 572, A92
Minchev I. et al., 2014b, ApJ, 781, L20
Nieva M.-F., Przybilla N., 2012, A&A, 539, A143
Nordström B. et al., 2004, A&A, 418, 989
Pagel B. E. J., 1997, Nucleosynthesis and Chemical Evolution of Galaxies. Cambridge Univ. Press, Cambridge
Pagel B. E. J., Patchett B. E., 1975, MNRAS, 172, 13
Radburn-Smith D. J. et al., 2012, ApJ, 753, 138
Rix H.-W., Zaritsky D., 1995, ApJ, 447, 82
Robin A. C., Reylé C., Derrière S., Picaud S., 2003, A&A, 409, 523
Roškar R., Debattista V. P., Quinn T. R., Stinson G. S., Wadsley J., 2008, ApJ, 684, L79
Schönrich R., Binney J., Dehnen W., 2010, MNRAS, 403, 1829
Sellwood J. A., 2014, Rev. Mod. Phys., 86, 1
Sellwood J. A., Binney J. J., 2002, MNRAS, 336, 785
Sellwood J. A., Carlberg R. G., 2014, ApJ, 785, 137
Sellwood J. A., Kahn F. D., 1991, MNRAS, 250, 278
Sharma S. et al., 2014, ApJ, 793, 51
Siebert A. et al., 2011, AJ, 141, 187
Smartt S. J., Rolleston W. R. J., 1997, ApJ, 481, L47
Solway M., Sellwood J. A., Schönrich R., 2012, MNRAS, 422, 1363
Spitoni E., Matteucci F., Recchi S., Cescutti G., Pipino A., 2009, A&A, 504, 87
Spitzer L., Jr, Schwarzschild M., 1953, ApJ, 118, 106
Springel V., Frenk C. S., White S. D. M., 2006, Nature, 440, 1137
Steinmetz M. et al., 2006, AJ, 132, 1645
Tacconi L. J. et al., 2013, ApJ, 768, 74
Vera-Ciro C., D'Onghia E., Navarro J., Abadi M., 2014, ApJ, 794, 173
Wakker B. P., 2001, ApJS, 136, 463
Whitford A. E., Rich R. M., 1983, ApJ, 274, 723
Worley C. C., de Laverny P., Recio-Blanco A., Hill V., Bijaoui A., Ordenovic C., 2012, A&A, 542, A48
Wyse R. F. G., Silk J., 1989, ApJ, 339, 700
Yanny B. et al., 2009, AJ, 137, 4377
Yoachim P., Roškar R., Debattista V. P., 2012, ApJ, 752, 97
Yoshii Y., 1981, A&A, 97, 280
Zwitter T. et al., 2008, AJ, 136, 421

This paper has been typeset from a TEX/LATEX file prepared by the author.